

Short Communication

Improving the Properties of Lithium Metal Batteries via Constructing of CuO nanowire array on Copper Foil (CuO NWA/Cu) as 3D Current Collector

Jingwen Ai¹†, Gaoxu Huang²†, Yuming Zhao¹, Qing Ding¹, Yuzhen Zhao^{3,*}, Shun Tang³, Guangbin Zhu³, Yuan-Cheng Cao³

¹ Electric Power Research Institute of Shenzhen, Shenzhen 518000, P. R. China

² Key Laboratory of Optoelectronic Chemical Materials and Devices, Ministry of Education, School of Chemical and Environmental Engineering, Jiangnan University, Wuhan 430056, P. R. China

³ State Key Laboratory of Advanced Electromagnetic Engineering and Technology, School of Electrical and Electronic Engineering, Huazhong University of Science and Technology, Wuhan 430074, P. R. China

†These authors contributed equally to this work.

*E-mail: zyz_272039252@sina.com

Received: 7 November 2019 / Accepted: 28 December 2019 / Published: 10 February 2020

Lithium metal batteries (LMBs) are promising energy storage system due to the lowest reduction potential and high specific capacity. However, the uncontrolled growth of Li dendrites during cycling processes might induce the low coulombic efficiency and severe safety hazards. Herein, our work focus on improving the performances of lithium metal batteries by constructing a new 3D current collector decorated with CuO nanowire array (CuO NWA@Cu). As a result, in contrast to the coulombic efficiency (about 90%) and voltage hysteresis (about 100 mV) of planar Cu after 10 cycles, the obtained CuO NWA@Cu has a higher coulombic efficiency (close to 98%) and lower voltage hysteresis (about 50 mV) at the current density of 0.5 mA cm⁻² after 100 cycles. This work provides a simple and scalable method to obtain CuO NWA@Cu 3D anode current collector for dendrite-free and high coulombic efficiency LMBs.

Keywords: Lithium metal batteries; CuO nanowire array; Anode; Coulombic efficiency

1. INTRODUCTION

The pursuit for batteries with high energy density and power output has inspired a revisit to the use of lithium (Li) metal anode which is featured with a high theoretic gravimetric capacity (3860 mAh g⁻¹) and low electrochemical potential (-3.04 V vs the standard hydrogen electrode)[1-3]. However, the uncontrolled growth of Li dendrites upon cycling might give rise to low coulombic efficiency and severe safety hazards, limiting its direct use[2-5]. In recent years, many methods have

been employed in stabilizing the Li anode of batteries[6,7], such as optimizing the liquid electrolytes by adding additives (FEC[8], DMTFA[9] etc.) and Li salts (LiNO₃[10], LiTFSI[11] etc.) for stabilizing interfaces between the Li metal and electrolyte[12,13], constructing the artificial protective layers (Li₂CO₃/C[14], Al₂O₃-PVDF-HFP[15] etc.) for suppressing the Li dendrites[16-19], using the proper Li alloys (LiAl[3], Li₁₃In₃[20] etc.) for decreasing lithium reaction activity[21,22] and so on. Although these studies have contributed to improving the stability of Li metal anodes, the dendrite-forming deposition nature of Li metal has hardly been changed.

The current density is one of the important factors affecting lithium deposition behavior[2,23,24]. 3D or nano-structured current collectors contribute to solving the Li dendrites partially due to 3D structure can decrease the local current density and regulate the electrical field distribution to allow uniform Li deposition[2,22,25-28]. Yang et al reported a g-C₃N₄@Ni which was used as three-dimensional anode current collector to improve lithium metal battery performance significantly[27]. Lu et al also reported a Cu@Ni core-shell nanowire anode current collector and the growth of lithium dendrite was greatly suppressed[29]. Herein, we constructed a 3D CuO NAW@Cu current collector with a submicron skeleton and high surface area in a facile and scalable method, and its electrochemical properties were also studied as anode for lithium ion battery.

2. EXPERIMENTAL

2.1. Preparation of self-supporting porous CuO nanowire array on the surface of Cu current collector (CuO NWA@Cu)

A copper (Cu) foil (9 μm in thickness) was firstly stamped into circular disks with a diameter of 14 mm, and then washed with acetone, ethanol, diluted HCl and deionized water for several times under ultrasonic to remove surface impurities and oxides. The pretreated Cu foils were immersed into a 30 mL aqueous solution containing 0.913 g (NH₄)₂S₂O₈ and 3.2 g NaOH at room temperature for 20 min. Then the samples were taken out and washed with deionized water for several times and then dried in air at room temperature. After that, the samples obtained were placed in a tube furnace and heated to 300 °C at a heating rate of 2 °C min⁻¹ and held for 2 h. The schematic representative of the synthesis of 3D porous CuO NWA@Cu current collector is shown in Fig.1.

2.2. Materials characterizations

X-Ray diffractometer (XRD, D/MAX 2500, Rigaku) was equipped with Cu K α radiation was used to characterize the composition and structure of obtained current collector. A scanning electron microscope (SEM, Hitachi, S-4700) operating at 3 kV was employed to observe the morphology of sample. The CuO NWA@Cu and planar Cu foil used as current collectors were assembled in CR2032 coin cells with Li metal as the reference and counter electrode to evaluate the electrochemical performance, respectively. The electrolyte was 1 M lithiumbis(trifluoromethanesulfonyl)imide (LiTFSI) in the solution of 1,3-dioxolane (DOL) and 1,2-dimethoxyethane (DME) (volume ratio:1:1, 80 μL) with 1% LiNO₃ as the additive. The Celgard2400 polypropylene membrane was used as separator. These batteries were assembled in an Ar-filled glove box and tested by a multi-channel battery testing system (Land 2001A Battery Testing System). To test the coulombic efficiency, a fixed

amount of Li (1 mAh cm^{-2}) was deposited on the current collector and then stripped until the voltage reaches 1 V (vs Li^+/Li) at 0.5 mA cm^{-2} or 1 mA cm^{-2} for each cycle, respectively.

3. RESULTS AND DISCUSSION

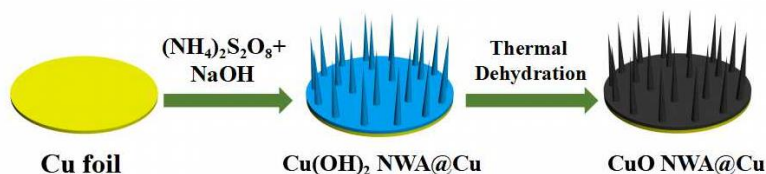


Figure 1. The Schematic representative of synthesis of 3D porous CuO NWA@Cu current collector

The morphologies of $\text{Cu}(\text{OH})_2 \text{ NWA@Cu}$ and CuO NWA@Cu is shown in Fig.2. The 3D structured $\text{Cu}(\text{OH})_2 \text{ NWA@Cu}$ (Fig.2 a, b, c) is composed of bundles of $\text{Cu}(\text{OH})_2$ fibres with $0.3 \mu\text{m}$ diameter. 3D $\text{Cu}(\text{OH})_2 \text{ NWA@Cu}$ is calcined to obtain 3D CuO NWA@Cu (Fig.2 d, e, f). The CuO NWA@Cu is thinner than the former, and the CuO submicron fibres (about $0.2 \mu\text{m}$) are roughly perpendicular to the foil, forming a jungle-like porous layer, and the uniform surface without secondary structure is more conducive to uniform deposition of lithium, which is close or superior to previous reports[2,25].

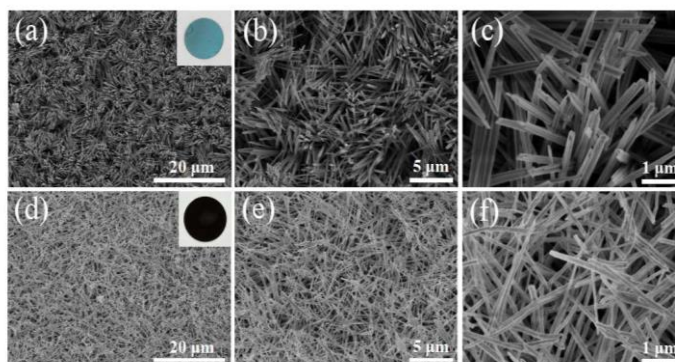


Figure 2. SEM images of $\text{Cu}(\text{OH})_2 \text{ NWA@Cu}$ (a, b, c) and CuO NWA@Cu (d, e, f) at different magnifications.

The structure of the CuO NWA@Cu and $\text{Cu}(\text{OH})_2 \text{ NWA@Cu}$ was characterized by XRD, as shown in Fig.3. The black XRD peaks show the mid-product (before calcination) on the surface of Cu foil is mainly $\text{Cu}(\text{OH})_2$ according to the typical peaks of $\text{Cu}(\text{OH})_2$ located at 32.4° , 35.5° and 38.7° , which are assigned to the (002), (111) and (130) lattice planes of $\text{Cu}(\text{OH})_2$ (PDF#13-0420)[2,25]. Simultaneously, the red (after calcination) show the typical peaks of $\text{Cu}(\text{OH})_2$ disappear and the peaks located at 35.5° and 38.9° start to appear, which are assigned to the (002) and (200) lattice planes of CuO (PDF#45-0937), and the same peaks located at 43.3° , 42.7° , 17.1° are assigned to the (111), (200) and (220) lattice planes of Cu (PDF#85-1326), which indicates that the CuO is grown on the surface of Cu foil[2,25].

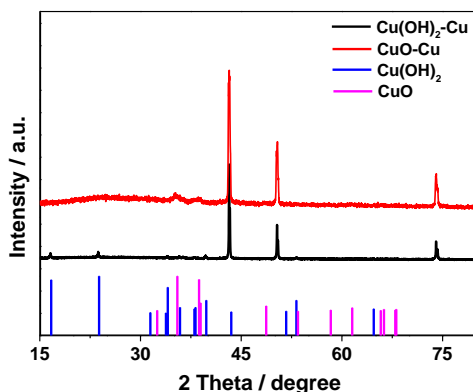


Figure 3. XRD patterns of $\text{Cu}(\text{OH})_2$ NWA and CuO NWA

The CEs of planar Cu foil and CuO NWA@Cu electrodes cycled with fixed 1 mAh cm^{-2} as shown in Fig.4 (a, b). The CE of CuO NWA@Cu is close to 98% (average CE is close to 96%) after 100 cycles at a current density of 0.5 mA cm^{-2} , much higher than that of the planar Cu foil (CE is close to 75% and average CE is close to 90% after 50 cycles). Especially, the CE of CuO NWA@Cu is about 95% (average CE is close to 93%) after 100 cycles at a current density of 1 mA cm^{-2} , however the CE of planar Cu foil is closed to 62% (average CE is close to 78%) after 50 cycle. Here, we compare the CE values of similar 3D current collector materials used in lithium batteries[25,26,30-35], and the CE value of CuO NWA@Cu in this paper is close to or better than other 3D current collector materials in the literature, as shown in Table 1. Therefore, CuO NWA@Cu is a anode current collector with better stable cycle performance. This may be attributed to the jungle-like porous 3D structure of CuO NWA@Cu with submicron framework, and a large amount of protruding tips on the submicron fibres as the charge centres and nucleation sites[2,25]. The electric field is roughly uniform and the charges are evenly distributed along the Cu framework[2,25]. Meanwhile jungle-like porous structure of CuO NWA@Cu contribute to decreasing the effective current density, thereby inhibiting the growth of Li dendrites. In addition, the porous structure can also effectively alleviating the volume expansion caused by repeated plating/stripping of lithium, further improving battery performance[2,25,30].

Fig.4 (c) and (d) show the voltage profiles of Li plating/stripping on planar Cu and CuO NAW@Cu, respectively. The voltage hysteresis of a planar Cu foil is about 100 mV after 10 cycles, while the voltage hysteresis of the CuO NAW@Cu is as low as 50 mV after 100 cycles at the current density of 0.5 mA cm^{-2} . The voltage polarization of the CuO NAW@Cu electrodes is much smaller than that of the planar Cu foil, which is close to or superior than the reported results in previous literatures[2,16,17,25]. Meanwhile it also indicates a much more stable Li plating/stripping process on CuO NAW@Cu than that of planar Cu foil. This result could be attributed to the fact that the jungle-like porous 3D structured CuO NAW@Cu has a larger specific surface area than that of the planar one[2,25]. The larger electroactive area can offer a larger interface of Li/electrolyte, lower the actual current density, and decrease the charge transfer resistance upon cycling compared with the planar one[2,25]. The low hysteresis of the Li anode is beneficial to decrease the voltage polarization during cycling, and improve the cyclic stability of lithium plating/stripping[2,25].

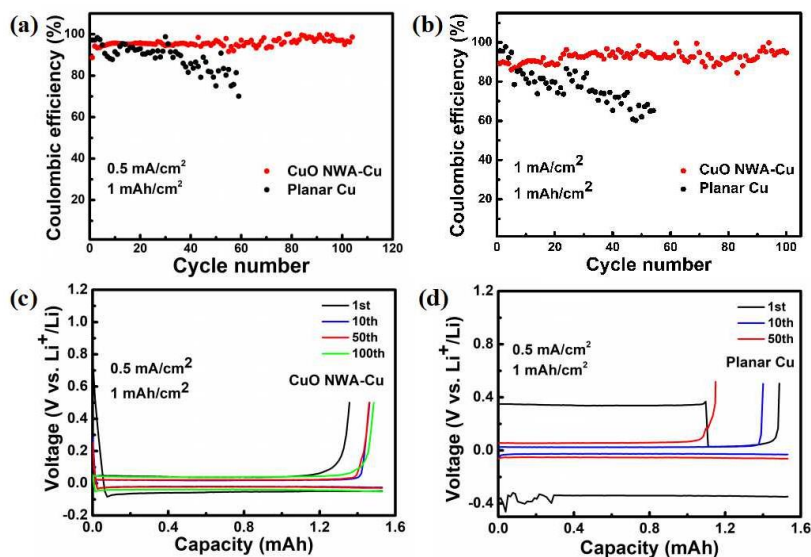


Figure 4. CE value of Cu and CuO NWA@Cu electrodes with a fixed lithium deposited amount of 1 mAh cm^{-2} at the different current density of (a) 0.5 mA cm^{-2} and (b) 1 mA cm^{-2} during Li plating/stripping process; Voltage profiles of the Li plating/stripping cycle on (c) CuO NWA@Cu and (d) planar Cu electrodes at different cycles at a current density of 0.5 mA cm^{-2} with a fixed lithium deposited amount of 1 mAh cm^{-2} .

Table 1. CE values of similar 3D current collector materials used in lithium batteries

Types of materials	Current density/ mA cm^{-2}	Number of cycles	CE	Reference
CuO NWA@Cu	1	100	95%	This work
3D LN	1	70	97%	Ref.30
CuZn mesh	1	70	60%	Ref.31
CGB	1	50	94%	Ref.32
GF	1	90	45%	Ref.33
AC/CNT	1	50	<95%	Ref.34
SS	1	100	<90%	Ref.26
SS/PIANC	1	140	88%	Ref.26
VA-CuO-Cu	1	180	94%	Ref.25
Cu foam	1	75	<90%	Ref.35

4. CONCLUSION

In summary, we described a facile and scalable strategy to prepare CuO nanowire array on the surface of Cu foil. When CuO NAW@Cu was utilized as the current collector of anode materials for lithium batteries, demonstrating good electrochemical performances with coulombic efficiency of 98% in a narrow voltage range at 1 mAh cm^{-2} after 100 cycles. Meanwhile the voltage hysteresis of CuO NAW@Cu is as low as 50 mV after 100 cycles at the current density of 0.5 mA cm^{-2} , and far below planar Cu foil (100 mV). These results indicate that CuO NAW@Cu would be a promising 3D current collector of anode materials for lithium metal batteries.

CONFLICTS OF INTEREST

There are no conflicts to declare.

ACKNOWLEDGMENTS

This project was supported by the fund from National Key R&D Program of China (2018YFB0905300, 2018YFB0905305) , Dr. Tang thanks the funds from Science and Technology Research Project of Hubei Education Department (B2017266) and China Southern Power research fund for fire safety assessments for large scale grid energy storage system (090000KK52190004).

References

1. J. M. Tarascon, M. Armand, *Nature*, 414 (2001) 359.
2. C. P. Yang, Y. X. Yin, S. F. Zhang, N. W. Li, Y. G. Guo, *Nat. Commun.*, 6 (2015) 8058.
3. S. L. Wu, Z. Y. Zhang, M. H. Lan, S. R. Yang, J. Y. Cheng, J. J. Cai, J. H. Shen, Y. Zhu, K. L. Zhang, W. J. Zhang, *Adv. Mater.*, 9 (2018) 1705830.
4. H. Kim, G. Jeong, Y. U. Kim, J. H. Kim, C. M. Parke, H. J. Sohn, *Chem. Soc. Rev.*, 42 (2013) 9011.
5. H. Ye, Z. J. Zheng, H. R. Yao, S. C. Liu, T. T. Zuo, X. W. Wu, Y. X. Yin, N. W. Li, J. J. Gu, F. F. Cao, Y. G. Guo, *Angew. Chem. Int. Ed.*, 58 (2019) 1094.
6. W. Xu, J. L. Wang, F. Ding, X. L. Chen, E. Nasybulin, Y. H. Zhang, J. G. Zhang, *Energy Environ. Sci.*, 7 (2014) 513.
7. J. M. Zheng, J. Tian, D. X. Wu, M. Gu, W. Xu, C. M. Wang, F. Gao, M. H. Engelhard, J. G. Zhang, J. Liu, J. Xiao, *Nano Lett.*, 14 (2014) 2345.
8. Q. C. Liu, J. J. Xu, S. Yuan, Z. W. Chang, D. Xu, Y. B. Yin, L. Li, H. X. Zhong, Y. S. Jiang, J. M. Yan, X. B. Zhang, *Adv. Mater.*, 27 (2015) 5241.
9. V. S. Bryantsev, V. Giordani, W. Walker, J. Uddin, I. Lee, A. C. T. Duin, G. V. Chase, D. Addison, *J. Phys. Chem. C*, 117 (2013) 11977.
10. W. Walker, V. Giordani, J. Uddin, V. S. Bryantsev, G. V. Chase, D. Addison, *J. Am. Chem. Soc.*, 135 (2013) 2076.
11. J. Qian, W. A. Henderson, W. Xu, P. Bhattacharya, M. Engelhard, O. Borodin, J. G. Zhang, *Nat. Commun.*, 6 (2015) 6362.
12. M. S. Park, S. B. Ma, D. J. Lee, D. M. Im, S. G. Doo, O. Yamamoto, *Sci. Rep.*, 4 (2014) 3815.
13. J. J. Hu, G. K. Long, S. Liu, G. R. Li, X. P. Gao, *Chem. Commun.*, 50 (2014) 14647.
14. M. Asadi, B. Sayahpour, P. Abbasi, A. T. Ngo, K. Karis, J. R. Jokisaari, C. Liu, B. Narayanan, M. Gerard, P. Yasaei, X. Hu, A. Mukherjee, K. C. Lau, R. S. Assary, F. K. Araghi, R. F. Klie, L. A. Curtiss, A. S. Khojin, *Nature*, 55 (2018) 502.
15. D. J. Lee, H. K. Lee, J. C. Song, M. H. Ryou, Y. M. Lee, H. T. Kima, J. K. Park, *Electrochem. Commun.*, 40 (2014) 45.
16. G. Y. Zheng, S. W. Lee, Z. Liang, H. W. Lee, K. Yan, H. B. Yao, H. T. Wang, W. Y. Li, S. Chu, Y. Cui, *Nat. Nanotech.*, 9 (2014) 618.
17. K. Yan, H. W. Lee, T. Gao, G. Y. Zheng, H. B. Yao, H. T. Wang, Z. D. Lu, Y. Zhou, Z. Liang, Z. F. Liu, S. Chu, Y. Cui, *Nano Lett.*, 14 (2014) 6016.
18. C. Huang, J. Xiao, Y. Y. Shao, J. M. Zheng, W. B. Bennett, D. P. Lu, S. V. Laxmikant, M. Engelhard, L. W. Li, J. G. Zhang, X. L. Li, G. L. Graff, J. Liu, *Nat. Commun.*, 5 (2014) 3015.
19. G. Q. Ma, Z. Y. Wen, M. F. Wu, C. Shen, Q. S. Wang, J. Jin, X. W. Wu, *Chem. Commun.*, 50 (2014) 14209.
20. X. Liang, Q. Pang, I. R. Kochetkov, M. S. Sempere, H. Huang, X. Q. Sun, L. F. Nazar, *Nat. Energy*, 2 (2017) 17119.
21. X. L. Zhang, W. K. Wang, A. B. Wang, Y. Q. Huang, K. G. Yuan, Z. B. Yu, J. Y. Qiu, Y. S. Yang, *J. Mater. Chem. A*, 2 (2014) 11660.
22. X. B. Cheng, H. J. Peng, J. Q. Huang, F. Wei, Q. Zhang, *Small*, 10 (2014) 4257.

23. C. Brissot, M. Rosso, J. N. Chazalviel, P. Baudry, S. Lascaud, *Electrochimica Acta*, 43 (1998) 1569.
24. C. Brissota, M. Rossoa, J. N. Chazalviel, S. Lascaudl, *Stud. Surf. Sci. Catal.*, 132 (2001) 947.
25. C. Zhang, W. Lv, G. M. Zhou, Z. J. Huang, Y. B. Zhang, R. Y. Lyu, H. L. Wu, Q. B. Yun, F. Y. Kang, Q. H. Yang, *Adv. Energy Mater.*, 8 (2018) 1703404.
26. W. Liu, D. Lin, A. Pei, Y. Cui, *J. Am. Chem. Soc.*, 138 (2016) 15443.
27. Z. Y. Lu, Q. H. Liang, B. Wang, Y. Tao, Y. F. Zhao, W. Lv, D. H. Liu, C. Zhang, Z. Weng, J. C. Liang, H. Li, Q. H. Yang, *Adv. Energy Mater.*, 9 (2019) 1803186.
28. Y. Q. Guo, X. F. Hong, Y. Wang, Q. Li, J. S. Meng, R. T. Dai, X. Liu, L. He, L. Q. Mai, *Adv. Funct. Mater.*, 29 (2019) 1809004.
29. L. L. Lu, Y. Zhan, Z. Pan, H. B. Yao, F. Zhou, S. H. Yu, *Energy storage materials*, 9 (2017) 31.
30. H. D. Liu, X. J. Yue, X. Xing, Q. Z. Yan, J. Huang, V. Petrova, H. Y. Zhou, P. Liu, *Energy Storage Materials*, 16 (2019) 505.
31. S. B. Huang, W. F. Zhang, H. Ming, G. P. Cao, L. Z. Fan, H. Zhang, *Nano Lett.*, 19 (2019) 1832.
32. S. Liu, A. X. Wang, Q. Q. Li, J. S. Wu, K. V. Chiou, J. X. Huang, J. Y. Luo, *Joule*, 2 (2018) 184.
33. B. Z. Yu, T. Tao, S. Mateti, S. G. Lu, Y. Chen, *Adv. Funct. Mater.*, 28 (2018) 1803023.
34. Z. W. Sun, S. Jin, H. C. Jin, Z. Z. Du, Y. W. Zhu, A. Y. Cao, H. X. Ji, L. J. Wan, *Adv. Mater.*, 30 (2018) 1800884.
35. Y. Y. Wang, Z. J. Wang, D. N. Lei, W. Lv, Q. Zhao, B. Ni, Y. Liu, B. H. Li, F. Y. Kang, Y. B. He, *ACS Appl. Mater. Interfaces*, 10 (2018) 20244.